Molecular Crystals and Liquid Crystals

Publication details, including instructions for authors and subscription information:
http://www.tandfonline.com/loi/gmcl16

AC and DC Regimes of the Electrohydrodynamic Instabilities in Nematic Liquid Crystals

Orsay Liquid Crystal Group [a]

[a] Laboratoire de Physique des Solides, 91-Orsay

Version of record first published: 21 Mar 2007.

To cite this article: Orsay Liquid Crystal Group (1971): AC and DC Regimes of the Electrohydrodynamic Instabilities in Nematic Liquid Crystals, Molecular Crystals and Liquid Crystals, 12:3, 251-266

To link to this article: http://dx.doi.org/10.1080/15421407108082778

Molecular Crystals and Liquid Crystals. 1971. Vol. 12, pp. 251–266

Printed in Great Britain

AC and DC Regimes of the Electrohydrodynamic Instabilities in Nematic Liquid Crystals†

ORSAY LIQUID CRYSTAL GROUP‡

Laboratoire de Physique des Solides
91–Orsay

Received October 31, 1970; *in revised form November* 23, 1970

Abstract—New experimental results on the electrohydrodynamic instabilities in nematics are presented. Joined with previously reported properties, they allow a general classification of these instabilities in term of one DC and two AC regimes. A quantitative explanation of the AC regimes is given, in the frame of the Carr-Helfrich model extended to time dependent phenomena.

Since the first experiments of Williams,[1] a large amount of work has been devoted to the study of electric instabilities in nematic liquid crystals (NLC). Potential applications of these effects have been explored for display purposes, mainly by the RCA Group.[2] In spite of these efforts, the understanding of the fundamental mechanisms governing these phenomena is yet far from complete. In particular, it seems that the DC and low frequency AC regimes have often been confused, because of their similar optical appearance. For these reasons, we have undertaken a systematic study of the electric instabilities in nematics under DC and AC excitation. Our present observations, together with previously reported results from several different groups, enable us to give a clear characterization of three distinct regimes of instabilities, leading to an assignment of the processes which are effective in each case. This will be dealt with in part 1 of this article. In part 2, we present a detailed quantitative discussion of our experimental results in AC excitation, comparing them with the theoretical prediction of a recent model.

† Presented at the Third International Liquid Crystal Conference in Berlin, August 24–28, 1970.

‡ Work supported by DRME, under contract n° 69/112.

1. Comparative Study of the DC and AC Instabilities of Nematics, Close to Threshold

After a brief description of our experimental conditions, we give some comments on our recent observations, and then try, in Table 1, to sum-up the main characteristic features of the different observed types of instabilities.

We use the experimental set up of Williams,[1] in which a cell of variable thickness e ($20\,\mu m < e < 240\,\mu m$) is made with two semi-transparent tin-oxyde coated electrodes and mylar spacers. The NLC used is the *p*-methoxy-*n*-*p*-benzilidene butylaniline (MBBA), oriented by rubbing, or by an applied magnetic field ($H \sim 20$ KG) which can be either parallel or perpendicular to the electrodes. We apply across the electrodes a DC voltage ($V < 100$ Volt), or an AC voltage in the range of frequency 10 Hz $< f <$ 3000 Hz, with RMS value limited to 500 V.

We observe the sample under a polarizing microscope. In this paper, we restrict ourselves to the lowest excitation regime, at the onset of the instabilities. In this case, all the optical patterns that we are going to describe are visible when the polarization of the incoming light is parallel to the molecular alignment; they vanish for perpendicular polarization (this is not true any more for higher excitation where the dynamic scattering mode[2] appears).

1.1. DC Excitation

Above a voltage threshold V_{th} of 5 V, one observes a periodic pattern, which may be hexagonal (see Fig. 1 in Ref. 3), linear or intermediate, depending on the surface state of the electrodes. These patterns are focal lines and visualize, via the flow birefringence, the existence of twin rotatory flows of opposite angular momentum,[3,4] which may interact to give the observed regular arrangement (Fig. 1). As first observed by Koelmans *et al.*,[5] these flows persist above T_c, the nematic→isotropic transition temperature. Within the accuracy of our measurements, there is no significant difference between the values of V_{th} above and below T_c.

In presence of a magnetic field H, one can distinguish two thresholds:[6]

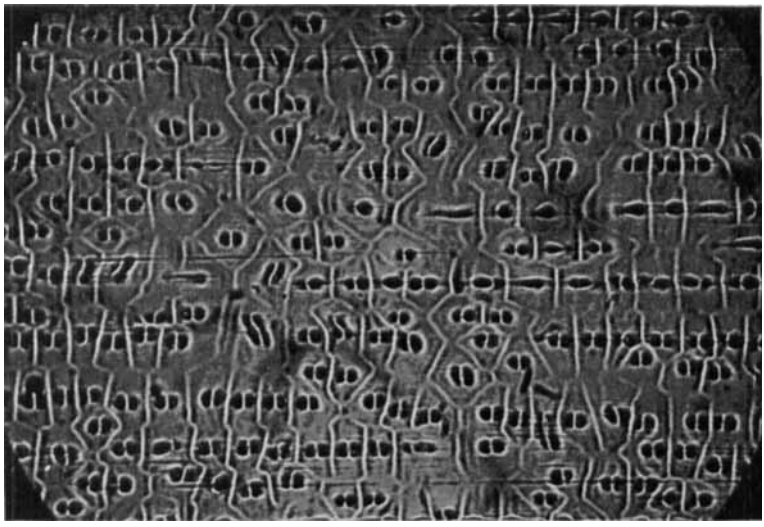

Figure 1. Typical microscopic appearance of the DC instability in MBBA ($V = 7$ volt). The twin dark spots are the coupled opposite hydrodynamic vortices. Notice that their axis are perpendicular to the rubbing direction (left to right) and that they attract to form linear chains before giving a more regular pattern—the size of each vortex is 50 μm (equal to the thickness of the nematic layer).

—the threshold of the hydrodynamical motion, which remains constant up to 20 KG;
—the threshold of the optical patterns, which increases with H, having the same value for parallel and perpendicular orientation.

This field effect can be simply understood: above V_{th}, hydrodynamic cellular motions develop, producing a shear induced torque destabilizing the molecules; the H field gives a stabilizing torque. Disalignment appears when the shear rate (and thus, the applied voltage) is large enough to beat the H field influence.†

On the whole, these observations suggest, for the instability, a mechanism which is not really specific of the anisotropic character of the mesophase. This is confirmed by the results of Gruler and Meier[7] in materials of positive and negative dielectric anisotropy.

† The hydrodynamical velocity is quadratic in the applied voltage (see Ref. 3); this leads to a linear increase of V_{th} with H which explains, with the correct order of magnitude, the observations of Rondelez (see Ref. 6).

In agreement with the experimental results of Heilmeier[2] we can infer that the DC instability is usually governed by some process related to charge carriers injection.

1.2. AC Excitation

Here, we have to distinguish two types of instabilities, depending on the values of the excitation frequency. They are characterized by the appearance of quite different optical patterns. The first regime, at low frequency, corresponds to the classical AC William striations; the visual aspect of the second one has not yet been described in the literature; but this higher frequency regime has been detected by Heilmeier and Helfrich[8] as a " fast turn off mode " in the dynaming scattering.

(a) *Low frequency regime*

As is well known, above a threshold voltage V_{th}, there appears a pattern of striations, perpendicular to the unperturbed direction of alignment of the molecules, with a period of the order of magnitude of the sample thickness e. It must be emphasized that the optical appearance is quite similar to the linear patterns of the DC excitation, and we observe the same array of hydrodynamic flows. However, this AC regime can be clearly distinguished from the DC one, through two recent observations of ours:

—the hydrodynamic motion vanishes above T_c.

—in the presence of an external field H, both the threshold for optical pattern and the threshold for hydrodynamic motion increase, but they always coincide.[6]†

It is also known that the threshold V_{th} increases with the frequency f of the AC field, up to a cut off frequency f_c; f_c has been shown to be proportional to the conductivity σ of the NLC.[8,9] In our experiments, f_c was varied from 50 Hz to 3000 Hz by doping the sample with ionisable molecules (tetramethyl ammonium halogenides).

(b) *Fast turn off mode*

Beyond the frequency cut off f_c, another type of optical pattern is observed, upon raising the applied voltage. It consists of parallel

† The observed relative increase of V_{th} with H (see Ref. 6) is of the order of e/ξ where ξ is the coherence length associated with H, in agreement with an Helfrich prediction (Ref. 11).

striations of much shorter period (a few μm) than the classical Williams striations, located in the middle plane of the NLC layer. They appear, at the threshold, perpendicular to the initial molecular alignment, but slightly above threshold they bend and move to give what we call " chevrons " (Fig. 2). This regime corresponds to the " fast turn off mode " previously quoted.[8]

Figure 2. Typical aspect of the AC instability in the dielectric regime (" chevrons ") in MBBA. $V = 260$ volt rms at 120 Hz. The distance between striations is 5 μm (thickness = 100 μm). Picture taken a few volts above threshold; the striations are grouped in ribbons which shift slowly in alternating directions. This is one type of a further instability above threshold not considered in the model.

Using samples of different thickness, we find a *field* threshold, E_{th}, in contrast with the voltage thresholds observed as well in the DC as in the AC low frequency regimes. E_{th} varies with the excitation frequency, following a parabolic law $E_{th} \simeq f^{1/2}$. An applied magnetic field does not change the value of the threshold, but increases the period of the striations (see part 2).

It is important to notice that, in the two AC regimes, charge carrier injection is not necessary for the onset of instabilities; we proved this point by using thin glass layers, insulating the electrodes

TABLE 1 Electric instabilities of nematic liquid crystals with *negative* dielectric anisotropy. ($\epsilon_a = \epsilon_\parallel - \epsilon_\perp < 0$). Notations: T_c, nematic → isotropic transition temperature; e, sample thickness; f, excitation frequency; σ: average conductivity.

	DC regime	AC regime	
		Low frequency:	Higher frequency:
Visual appearance	Williams striations[a] or cellular patterns†[b] period $\simeq e$	Williams striations[a] period $\simeq e$	parallel striations or " chevrons "†. period $\simeq$ a few μm†
	All striations perpendicular to the unperturbed molecular alignment, visibles when polarization of incoming light is parallel to the molecular alignment. Vanish for perpendicular polarization.		
Associated hydrodynamic behavior	Hydrodynamic cellular flows[c][d] Persist above T_c[e]	Hydrodynamic cellular flows[c][d] Vanish above T_c†	not observed not observed
Response time	Slow[f]	Slow[f]	" fast turn off " mode[g]
Thresholds:			
-nature	voltage threshold[f] $V_{th} \simeq 5$ volt	voltage threshold[f] $V_{th} \simeq 7$ volt (low frequency)	Electric field threshold† $E_{th} \simeq 25$ KV/cm at 100 Hz
	In absence of magnetic field, the thresholds for optical patterns and hydrodynamic flows are equals		
-frequency dependence		V_{th} increases up to cut off frequency f_c[a][f] $f_c \simeq \sigma$[g][h]	$E_{th} \simeq f^{1/2}$†

Influence of a magnetic field H:			
-optical pattern threshold	increases with H†	increases with $H^{(h)}$†	Independent of H†
-hydrodynamic *flow threshold*	independent of H†	keeps equal to optical *threshold* (increasing with H)†	
Necessity of charge carriers injection	yes[f]	no†	no†
Proposed responsible mechanisms	Combined effects of charge carriers injection and Carr[i] Helfrich[j] process[k]	Carr[i]-Helfrich[j] mechanism (for a detailed AC model see ref. 13 and 14)	

References: † Present work; part of these results constitutes the 3rd cycle thesis of one of us, F. Rondelez (Orsay, 1970) –(a) R. Williams, Ref. 1 (b) M. Hareng, private communication –(c) G. Durand, M. Veyssie, F. Rondelez and L. Leger, Ref. 3 –(d) A. Penz, Ref. 4 –(e) H. Koelmans and A. M. Van Boxtel, Ref. 2 –(f) G. Heilmeier, L. Zanoni and L. Barton, Ref. 2 –(g) G. Heilmeier and W. Helfrich, Ref. 8 –(h) D. Teaney and A. Migliori, Ref. 9 –(i) F. Carr, Ref. 10 –(j) W. Helfrich, Ref. 11 –(k) P. G. de Gennes, Ref. 12.

from the bulk NLC; we observe exactly the same phenomena as with conducting electrodes when equivalent voltages are applied across the NLC layer.

To conclude, we can infer that, in the AC regimes, the mechanism of instability is closely related to the existence of the nematic mesophase. All the observations are compatible with the Carr[10]–Helfrich[11] model, as recently extended to AC excitation.[13,14] This point will be discussed in more detail in part 2.

(c) For the sake of clarity, we present in Table 1 the main characteristics of the three types of instabilities, gathered from various sources, including the present observations, but restricted to nematics with negative dielectric anisotropy. Considering this table, one can see that the AC instabilities are now reasonably well understood.

As for the DC case, in spite of the well defined observed behavior, the injection mechanism is not clear, and necessitates further investigation, in particular on the role of the electrodes. The case of nematics with positive dielectric anisotropy has been less experimentally investigated, although it is considered in the AC model of Ref. (14). The very recent results of Gruler and Meier presented at this same conference also seem compatible in AC with the theoretical predictions.

2. Quantitative Description of the AC Instabilities of a Nematic Liquid Crystal

In part 1 we have given a qualitative description of the electrohydrodynamic instabilities of nematic liquid crystals. We have shown that, if injection must play a role for DC excitation, the two AC regimes can be explained by a mechanism closely related to the existence of the nematic mesophase. In a recent letter[13] we have demonstrated that the Carr–Helfrich[10,11] mechanism, extended to time depending phenomena, was adequate to describe the AC regimes. In this section we discuss quantitatively our results in the frame of this model; after a brief survey of the theory (Sec. 2.1), we compare the predictions of this model with our threshold measurements (Sec. 2.2); we then describe (Sec. 2.3) observations on the high field (dielectric) instability, which confirm the validity of the model.

2.1. Theoretical Model

Let us recall briefly the Carr–Helfrich mechanism.[11] Assume a NLC layer of uniform orientation, submitted to an external electric field E. An angular distortion ϕ of the nematic texture can be amplified through the following steps:

—a space charge q is created in the distorted regions, because of the existence of an anisotropic conductivity ($\sigma_a = \sigma_{\parallel} - \sigma_{\perp} > 0$; the subscript $\parallel$ and $\perp$ apply to the director of the NLC)

—the electric force ($\sim Eq$), acting on these space charges, induces hydrodynamic vortices.

—this hydrodynamic flow, coupled by viscous friction to the molecular alignment, increases the initial distortion ϕ. (Of course one has also to take into account the destabilizing effect of the transverse E field created by q.)

A structural instability arises when the electric excitation overcomes a threshold value, characteristic of the anisotropy of the NLC.

This model has been extended to time dependent phenomena.[13,14] Two regimes of instability are indeed predicted, according to the range of the frequency f of the AC excitation. At low frequency, in the " conducting regime ", space charges oscillate and drag the fluid, inducing the hydrodynamic motions described in part 1. A voltage threshold is predicted, with a frequency dependence given by

$$V_{th}^2 = V_H^2\{1 + (\zeta^2 - 1)(f/f_c)^2\}/\{1 - (f/f_c)^2\} \tag{1}$$

where V_H is the DC Helfrich voltage (Eq. 6, Ref. (11)), while f_c is a cut off frequency given by:

$$f_c = (\zeta^2 - 1)^{1/2}/2\pi\tau \tag{2}$$

ζ^2 is the " Helfrich " parameter, characteristic of the material, defined by:

$$\zeta^2 = \left(1 - \frac{\epsilon_{\parallel}}{\epsilon_a}\frac{1}{1 + \eta_0/\gamma_1}\right)\left(1 - \frac{\sigma_{\perp}\epsilon_{\parallel}}{\sigma_{\parallel}\epsilon_{\perp}}\right) \tag{3}$$

τ is the dielectric relaxation time:

$$\tau^{-1} = 4\pi\sigma_{\parallel}/\epsilon_{\parallel} \tag{4}$$

ϵ_a ($\epsilon_a = \epsilon_{\parallel} - \epsilon_{\perp}$) is the anisotropy of the dielectric constant. γ_1 is the twist viscosity[15]; η_0 is the averaged combination: $\eta_0 = (\eta_1 + \eta_2 - \gamma_1)/2$ of γ_1 and of the Miesowicz viscosity coefficients.[16]

Beyond f_c, at high field excitation, the second instability (the " dielectric " regime) occurs, for a field threshold E_{th}. When f is much larger than f_c, E_{th} is given by:

$$\langle E_{th}^2 \rangle = Af \tag{5}$$

with

$$A(\text{cgs, esu}) = \frac{8\pi^2}{|\epsilon_a|(1/\gamma_1 + 1/\eta_0)C(\zeta^2)} \tag{6}$$

$C(\zeta^2)$ is a dimensionless constant of the order of unity, tabulated in Ref. (14). In this regime, the NLC director undergoes angular oscillations.

2.2. Threshold Measurements

Let us now comment on our threshold measurements on the two AC regimes. Obviously the low frequency Williams striations correspond to the " conducting regime " and the " fast turn off mode " to the " dielectric regime ". On Fig. 3 we plot the observed threshold V_{th} versus f for a typical sample.

(a) *The conducting regime*

The experimental data for V_{th} are in reasonable agreement with the analytical form of Eq. (1) (full line I in Fig. 3) and allow a determination of the Helfrich parameter. For the 100 μm sample of Fig. 3, the ζ^2 value is 4.5 ± 0.5; systematic measurements from different samples give analogous values, but with an apparent dependence on e; ζ^2 varies slowly from 2.5 for the thinner samples ($e \sim 30\,\mu$m) up to 5 for the thicker samples ($e \sim 200\,\mu$m); these results are to be compared with the estimated value† 3 ± 0.5 from Eq. 3. The agreement between predicted and experimental values seems good for thin samples ($e < 50\,\mu$); the discrepancy for thicker samples may be understood by a systematic over-estimate of V_{th} due to the larger time constant for the onset of texture distortion (the time constant increases like e^2). For thin samples, there may be another source of error; spurious injection may influence our observations when the

† In this estimate, we use experimental data for dielectric constants and conductivity anisotropy in MBBA. (D. Diguet *et al.*, *Comptes Rendus*, **271B**, p. 954, 1970–.) The unknown ratio η_0/γ_1 is estimated between 0.25 and 0.5 by taking values from p.azoxyanisol (PAA) (Orsay Liquid Crystal Group, Third liquid crystal conference, Berlin, 1970).

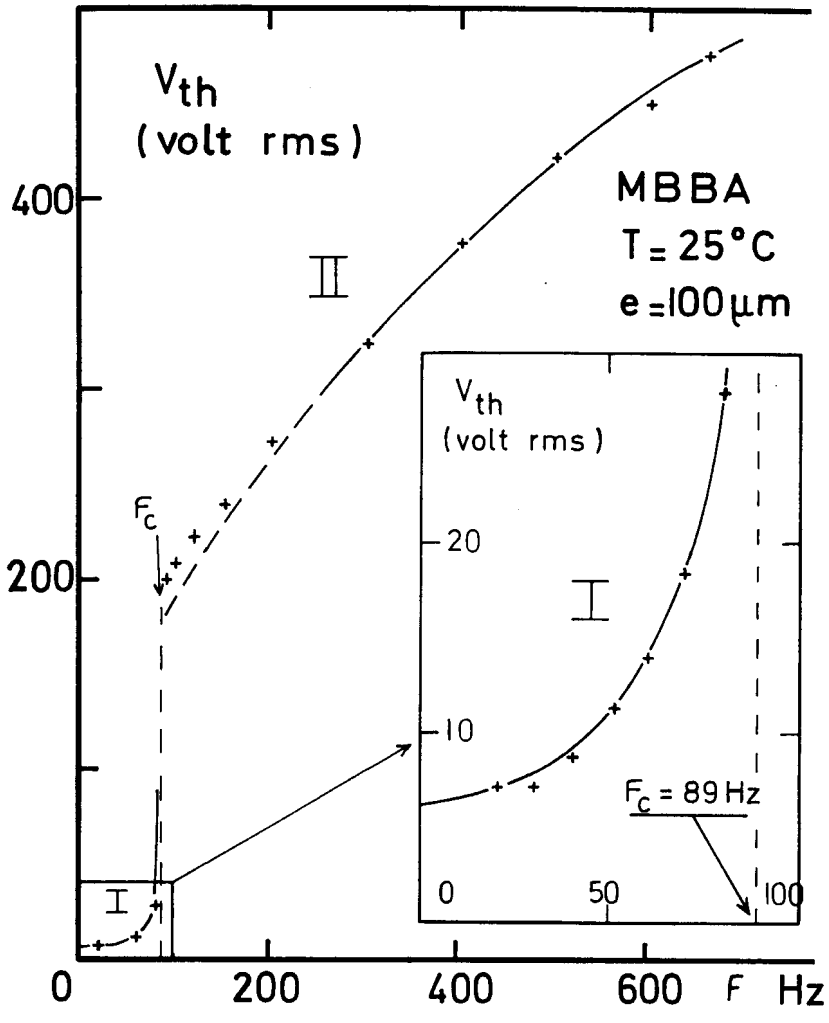

Figure 3. Voltage threshold V_{th} of the AC instabilities for MBBA. Region I: conducting regime (Williams striations); Region II: dielectric regime (" chevrons "); Full lines: theoretical curves from the AC extension of the Carr-Helfrich model (see text). [Figure taken from ref. 13.]

transit time of an ion across the NLC layer $e^2/\mu V$ is smaller than $1/2f$ where μ is the ion mobility; for MBBA at 25 °C, $\mu \sim 10^{-5}$ cm²/vs and $V \sim 10$ v give for the thinner samples ($e \sim 20\,\mu$m) a limiting frequency of 12 Hz, not very small compared to f_c (50 Hz $< f_c <$ 150 Hz). Spurious injection should become negligible above $e \sim 40\,\mu$m. Systematic measurements are under way to improve the determination of ζ^2.

In principle, one can also deduce ζ^2 from the coupled measurements of f_c and $\sigma_\parallel$ (Eqs. 2 and 4); unfortunately, in our unsealed cells, f_c is found to be one order of magnitude larger on the boundary of the NLC than in the uniform central region. This indicates a radial gradient of conductivity (close to the edges), which perturbs the determination of σ. By this method, we do find comparable values of ζ^2, but we cannot improve the accuracy of the previous measurements.

(b) *The dielectric regime*

Figure 3 shows a good agreement between the observed *field* threshold and the parabolic law of Eqs. 5 and 6 (full line, portion II), for $f > 3f_c$. The departure from the parabola, for f close to f_c, is expected theoretically and cannot by any means be attributed to injection, completely negligible in this regime with our present experimental conditions. From the experimental threshold field and the knowledge of the absolute viscosities in MBBA, one can determine the Helfrich parameter through the tabulated value of $C(\zeta^2)$ from Ref. (14). Using the previous estimate of η_0/γ_1 in PAA (see footnote, page 260) and assuming that they remain valid in MBBA, then calibrating the absolute viscosity from a recent measurement in MBBA,[17] we estimate $u = 1/\eta_0 + 1/\gamma_1$ to be in the range $u = 4 \pm 0.5$ cgs; this leads to: $C(\zeta^2) \sim 1$ and $\zeta^2 \sim 3$, which compares reasonably well with the expected value.

2.3. Further Studies on the Dielectric Regime

In this section, we present a measurement of the temporal and spatial dependence of the bending oscillations in the dielectric regime; for this purpose, we shine the sample with a parallel laser beam ($\lambda = 0.633\,\mu$m) normal to the plates and polarized parallel to the unperturbed nematic director. Above threshold, we observe intense Bragg scattered beams; from the scattering angle we derive

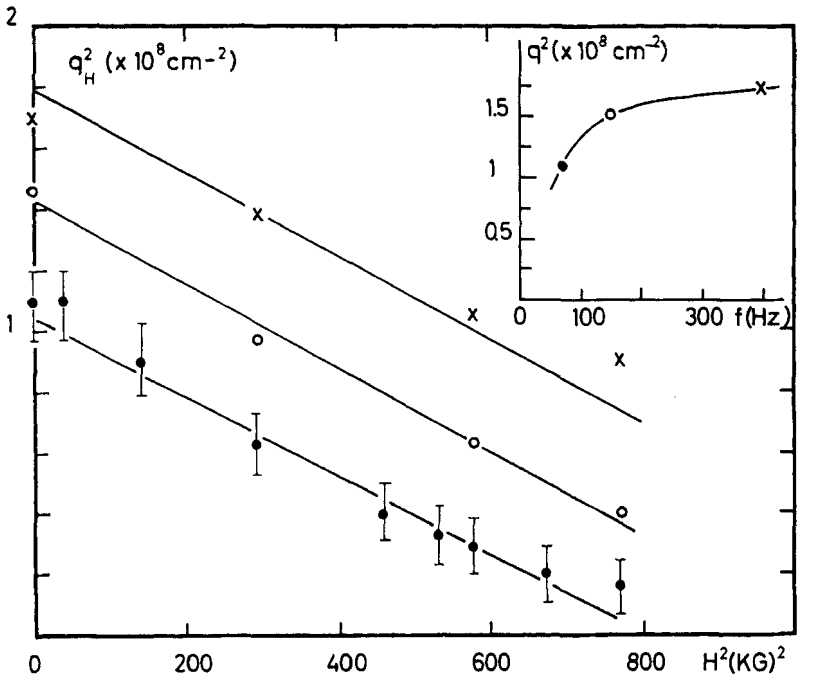

Figure 4. Dielectric regime: magnetic field dependence of the wave vector q_H of the bending oscillation for three different frequencies of excitation. The slope of the straight lines give the ratio $K_{33}/\chi_a = 9 \pm 2$ cgs. (see Eq. 7). In the upper corner, the corresponding plot of q^2 in zero H field, versus the excitation frequency. Note than q^2 increases less than expected, which is not yet understood—$e = 100$ μm.

the wave vector **q** of the angular oscillation; from the time dependence of the scattered intensity, we deduce $\phi(t)$.

(a) *Frequency dependence of q in absence of magnetic field*

The existence of a well defined wave vector for the bending oscillations in the dielectric regime is predicted in the model.[14] As stressed by de Gennes,[18] this means that in spite of the expense of elastic Franck energy ($K_{33}q^2/2$) associated with the bending, the nematic director can respond more easily to the high frequency excitation. The model predicts that the damping rate $K_{33}q^2/\eta$ of the bending mode remains proportional to the AC frequency, in absence of diffusion currents. Increasing f from 50 to 1000 Hz, we do observe an increase of $q^2(f)$ (Fig. 4) but less rapid than expected. This may be due to the too large resistivity of our samples. Further experiments will check this point.

(b) *Magnetic field dependence of q for constant frequency*

We apply the magnetic field **H** parallel to the director. The same argument on response times leads (for constant f) to the prediction:

$$K_{33} q_H^2 + \chi_a H^2 = K_{33} q^2 \tag{7}$$

where q_H is the bending wave vector at the field H and χ_a the anisotropic part of the diamagnetic susceptibility. Varying H from 0 to 28 KGauss, we first notice that E_{th} is independent of H. Figure 4 shows the plot of q_H^2 versus H^2 for three different q corresponding to different excitation frequencies; these results, in the limit of our present accuracy, verify Eq. (7) and give the value $K_{33}/\chi_a = 9 \pm 2$ cgs (MBBA, $T = 21.5\,^\circ$C, $e = 100\,\mu$m).

(c) *Anharmonicity of ϕ (t) above threshold*

The intensity of the laser light, Bragg scattered by the bending oscillation, is proportional (for small amplitudes ϕ) to $\phi^2(t)$. For MBBA, with a Helfrich parameter $\zeta^2 \sim 3$, one expects $\phi(t)$ to be significantly anharmonic[14] and, (in the limit of large excitation) to behave nearly as $1/\cos 2\pi ft$, postulating the validity of the model

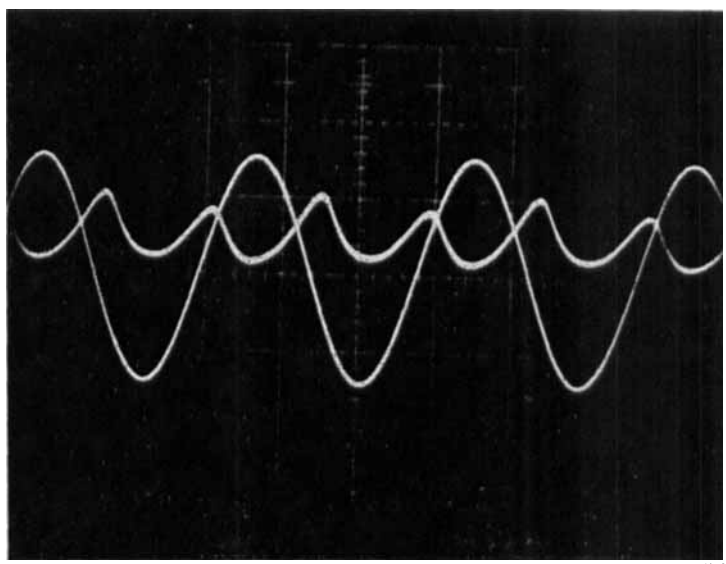

Figure 5. Synchronous recording of the excitation field (sine wave) and of the scattered light intensity in the first Bragg beam (arbitrary scales). Note the anharmonicity of the light intensity, which peaks when the E field goes to zero.

above threshold. Figure 5 shows a synchronous recording of the exciting sine wave electric field, and of the intensity of the first order beam diffracted by the NLC layer which acts as an optical grating. One observes that the maximum scattered intensity, as expected, peaks when the E field goes to zero. A more detailed numerical analysis of $\phi(t)$ is under way.

Conclusion

Since the last liquid crystal conference (Kent 1968), the understanding of the electric instabilities in nematics has considerably improved from both experimental and theoretical points of views. There is now a satisfactory description of the AC regimes which appear to be specific of the mesophase. The DC instability is recognized to be a closer parent of the electro-hydrodynamic phenomena observed in normal insulating fluids submitted to unipolar charge injection.[19]

A few questions remain unanswered but should be hopefully clarified in the near future; among them, the important problem of the DC injection mechanism.

Finally, we would like to emphasize that all the properties we have described in this paper characterize the NLC instabilities in the vicinity of the threshold. For the technological applications, such as " display ", one has to force the system far beyond the threshold, in a turbulent regime (the " Dynamic Scattering " mode), which appears as a further instability of the presently described instabilities. The corresponding hydrodynamical problem is yet far from being resolved.

REFERENCES

1. Williams, R., *J. Chem. Phys.* **39,** 384 (1963).
2. Heilmeier, G., Zanoni, L. and Barton, L., *Proc. IEEE* **56,** 1162 (1968).
3. Durand, G., Veyssie, M., Rondelez, F. and Leger, L., *Comptes Rendus* **270B,** 97 (1970).
4. Penz, P. A., *Phys. Rev. Let.* **24,** 1405 (1970).
5. Koelmans, H. and van Boxtel, A. M., *Phys. Let.* **32A** 32 (1970).
6. Rondelez, F., 3rd cycle thesis, Orsay (1970).
7. Gruler, H. and Meier, G., Liquid Crystal Conference, Berlin (1970).
8. Heilmeier, G. and Helfrich, W., *Appl. Phys. Let.* **16,** 1955 (1970).

9. Teaney, D. and Migliori, A., IBM Report n° RC 2672 (Oct. 1969) *J. Appl. Phys.* **41**, 998 (1970).
10. Carr, E. F., *Mol. Cryst.* **7**, 253 (1969).
11. Helfrich, W., *J. Chem. Phys.* **51**, 4092 (1969).
12. de Gennes, P. G., *Comments on Solid State Physics*, part I, to be published.
13. Orsay Liquid Crystal Group, *Phys. Rev. Let.* **25**, 1642 (1970).
14. Dubois-Violette, E., de Gennes, P. G. and Parodi, O., *J. Physique*, to be published (April 1971).
15. Orsay Liquid Crystal Group, *Phys. Rev. Let.* **22**, 1361 (1969).
16. Miesowicz, M., *Nature* **158**, 27 (1946).
17. Martinoty, P., Thesis, Strasbourg (1970).
18. de Gennes, P. G., *Comments on Solid State Physics*, part II, to be published.
19. Felici, N., *Rev. Gen. Elect.* **78**, 717 (1969).